Developing PbSe/PbS Core-Shell Nanocrystals Quantum Dots (NQDs) for NQD/Silicon Heterojunctions

Jian Xu, Dehu Cui, Shengyong Xu, Gary Paradee, Fan Zhang, and Ting Zhu

The Pennsylvania State University
State College, PA, USA, jianxu@engr.psu.edu

ABSTRACT

We report in this paper the epitaxial growth of PbS shells over PbSe nanocrystal quantum dots (NQDs) with monolayer-precision. The core-shell infrared NQDs were ligand-exchanged with short-chain octadmine, and the photoluminescence efficiency of the surface-engineered core-shell nanoparticles was substantially higher than that of the plain core structures undergoing the same surface processing, which reveals less ligand-dependence and enhanced chemical robustness in the core-shell NQDs. The reported results could potentially open up the possibility of incorporating semiconductor infrared NQDs in the silicon matrix to develop all-inorganic light emitting heterojunctions on silicon substrates.

Keywords: colloidal nanocrystals, quantum dots, photoluminescence, infrared, light emitting devices.

1 INTRODUCTION

The newly developed colloidal nanocrystals of IV-IV compounds are currently receiving widespread attentions due to their unique electronic structures and superior optical properties [1-6]. The quantized electronic transitions in Pb(S,Se) NQDs have been reported to provide size-tunable interband absorption and luminescence emission at a broad and technically important infrared wavelength range, spanning 0.8 μm to 4.0 μm [7]. Sharp exciton absorption features and high photoluminescence (PL) efficiency (~89%) of PbSe NQDs have been reported [8]. Tunable optical gain and amplified spontaneous emission have been observed from PbSe nanocrystal films [9]. Electroluminescence devices based on Pb(S,Se) NQDs were demonstrated recently with a size-tunable infrared emission between 1.0 μm and 2.0 μm, and high external quantum efficiencies up to 3% [10-12].

The emergence of the high-quality infrared NQDs also opens the possibility of incorporating semiconductor infrared NQDs in the silicon matrix to develop all-inorganic light emitting heterojunctions on silicon substrates. Such a heterojunction will comprise layers of infrared quantum dots embedded at the interface of a silicon p-n junction to form the intrinsic active region of a light emitting diode (LED). Since PbSe NQDs and the crystalline silicon form overlapping Type-I heterojunctions at the interface ($E_{gNQD} \leq 1.0$ eV), the free-carrier injection into PbSe nanocrystals is energetically favored from the wider band-gap silicon cladding layers. Electrons and holes will be injected, via n- and p-regions of the silicon junction, into the embedded NQDs, where the radiative recombination leads to the excitonic emission with quantum-enhanced efficiency and size tunable wavelengths. Since silicon is largely transparent to the infrared light ($\lambda \geq 1100$nm), the heterojunction will transmit the infrared emission from the NQD-active region with low losses.

The NQD-silicon integration scheme is, however, hindered by the fact that the as-prepared PbSe nanoparticles are overcoated with a layer of oleate ligands which function to passivate the surface traps as well as keeping NQDs from agglomerating in organic solvents [13]. The long-chain nature of the surfactant molecules poses barriers to the free-carrier transport between the guest NQDs and the host silicon layer, and introduces structural defects at NQD-NQD and NQD-silicon interfaces [14]. The technique of ligand exchange could potentially provide the ultimate solution to this problem by replacing the long-chain ligands with conductive or "good-leaving" molecules which are readily removed from NQD thin films by vacuum-heating, leaving a layer of surface-engineered NQDs for the subsequent overgrowth of the semiconductor capping layer [15]. Nevertheless, successful ligand exchange has so far only been achieved on nanoparticles of core-shell architectures, such as CdSe/CdS and CdSe/ZnS core-shell NQDs of the visible emission wavelength. The wider band-gap (Zn,Cd)S shells effectively passivate and protect the radiative CdSe cores during the "ligand removal" process, whereas those NQDs of plain core structures often lose their emissivity substantially due to the degradation of the unprotected surfaces in the reaction.

We report in this paper the epitaxial growth of PbS shells over PbSe NQDs with monolayer precision. The core-shell infrared NQDs were ligand-exchanged with short-chain octadmine, and the photoluminescence efficiency of the surface-engineered core-shell nanoparticles was substantially higher than that of the plain core structures

undergoing the same surface processing, which reveals less ligand-dependence and enhanced chemical robustness in the core-shell NQDs. While there has been a report on the successful synthesis of PbSe/PbS NQDs, the tributylphosphine/trioctylphospine (TBP/TOP) surfactant-based synthetic approach reported by Brumer *et al.* produced PbSe NQDs of lower quantum-efficiency (~40%) than those prepared with oleate ligand–based approach (~85%). In addition, there were no disclosed information on the ligand dependence, chemical stability and processibility of the synthesized core-shell structures yet.

2 SAMPLE PREPARATION

In this study, PbSe NQDs of plain core structures were synthesized following the noncoordinating solvent technique developed by Yu *et al [3]*. The as-prepared PbSe nanostructures were stabilized with a capping layer of oleate molecules coordinated to the Pb atoms. High-resolution transmission electron images of the synthesized NQDs show well resolved regular lattice fringes without detectable stacking fault and other internal defects, indicating the single crystalline-domain in the nanoparticles. The interband absorption spectra of 6nm-NQDs exhibit sharp excitonic absorption features which are discernable up to the second order. Room-temperature PL from the PbSe solution is strong and exhibits small Stokes shifts, indicative of a dominant band-edge emission. The full width at half maximum (FWHM) bandwidth of the PL emission of 6nm-NQDs is 158 nm.

The technique of successive ion layer adsorption and reaction (SILAR) [16], originally developed for the deposition of thin films on solid substrates from solution baths, has been adapted to the growth of high-quality PbSe/PbS core-shell nanocrystals. While Peng *et al*. has adopted such a synthetic approach to grow wider bandgap shells over II-VI NQDs with an impressive success, efforts were taken to apply the SILAR technique to the IV-VI NQD system due to the different compound families and coordinating ligands involved in the synthesis. In order to gain the monolayer-control over the shell formation, cationic and anionic precursors, Pb^{2+} and S^{2-}, were injected alternatively into the reaction mixture with core nanocrystals. The dosage of each injection was precisely controlled such that one-half of a shell-monolayer will grow epitaxially over PbSe plain cores following each addition of either cationic or anionic reagents. Since there was little opportunity for the cationic and anionic species to coexist with each other in the reaction solution, the direct nucleation of the shell-compound into cores was avoided.

During the SILAR synthesis, highly fluorescent PbSe nanocrystals were first purified by mixing with bad solvent (acetone), centrifuge-precipitating and decantation. The PbSe nanocrystals were then diluted in Octadecene (ODE), heated to ~140°C in a three-neck flask. A lead-injection solution was prepared by mixing PbO, Oleic acid and ODE in the second three-neck flask, heated to ~157°C under the argon flow to obtain a colorless clear solution. The sulfur-injection solution was prepared by dissolving sulfur in TOP (Trioctylphosphine) and ODE, then sonicating the mixture in ultrasonic bath to get a clear solution. The temperature of lead-injection solution was retained at ~80 °C, whereas the sulfur-injection solution was allowed to cool to room temperature.

The shells were grown epitaxially, one monolayer at a time, by the consecutive syringe-injection of the predetermined dosages of lead- and sulfer- solutions into the preheated PbSe-core solution using the standard air-free procedure. The amount of lead and sulfur precursors required for the first shell-layer growth was determined by the size and the lattice structure of the PbSe plain cores employed in the synthesis. The reaction temperature was kept at 140 °C, below that required for the nucleation of individual PbS nanocrystals. To monitor the reaction, aliquots were taken 1-5 min after every two successive injections of lead and sulfur solutions for the absorption and PL measurements. When the desired number of shell layers was reached, the reaction mixture was cooled to terminate the reaction. In this approach PbSe/PbS NQDs of 1-5 shell layers have been synthesized. According the lattice constants of bulk PbS and PbSe crystals, there is a 3.1%-tensile strain in PbS-shell layers epitaxially grown over PbSe plain cores. The calculated critical thickness substantially exceeds the thickness of 1-5 layers of PbS shells, which excludes the concern of any strain related dislocations in our investigation of II-VI core-shell structures.

3 CHARACTERIZATION AND ANALYSIS

The final product was diluted by chloroform followed by a methanol extraction. Excess ligands were further removed by repeatedly precipitating the core-shell NQDs with acetone and eventually dispersed in chloroform for storage. A small portion of the nanocrystals were re-dispersed in tetrachloroethylene for NIR absorption and PL measurements. The PL spectroscopy of PbSe/PbS NQDs was characterized with a CM110 Spectralproducts NIR spectrometer and a 904nm-diode laser module as the excitation source.

Figure 1 shows the evolution of PL spectra of the core-shell NQDs upon the growth of PbS shell in a typical reaction. A consistent red-shift of the peak wavelength was observed from the PL spectra upon the increase of the number of shell layers. Similar shifts of wavelength were also observed by Steckel and Peng *et al.* during the synthesis of CdSe/CdS core-shell NQDs. We believe that the increased layer number of PbS shells reduces the quantum confinement on the electronic transitions in PbSe

nanocrystals due to the relatively low barrier height at PbSe/PbS interface (~0.1 eV) and renders the spreading of the carriers' wavefunctions out of the core regions, which in turn leads to the observed red shift of the optical transition with respect to the plain core samples. The intensity variation of the sample PL during the overgrowth

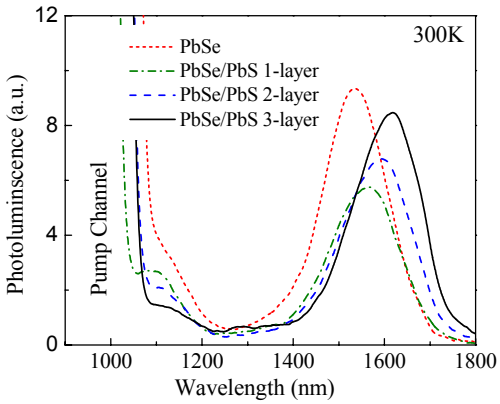

Figure 1. The evolution of the PL spectra of core-shell PbSe-PbS nanocrystals upon the growth of PbS shell in the chemical synthesis.

of PbS shells exhibits an initial fall and the subsequent increment up to the forth layer, which corresponds to 85% of the maximum quantum efficiency of plain core PbSe NQDs. Upon the growth of thicker PbS shells, the PL intensity of the sample starts to decline again.

The epitaxial growth of the core/shell structures was verified by high resolution transmission electron microscopy (TEM) (Fig. 2). The well resolved lattice

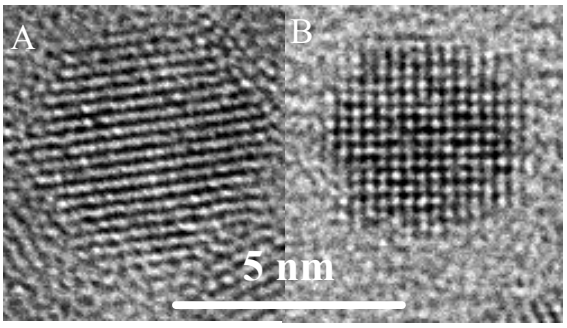

Figure 2. High resolution TEM image of PbSe nanocrystals (a) with and (b) without three monolayers of PbS shells.

fringes are continuous throughout the entire particle, indicative of the epitaxial nature of the shell-growth. In comparison with spherical NQDs of plain cores, the core-shell PbSe NQDs exhibit larger size with slightly elongated shape. While monodispersed plain core NQDs often form well ordered 2D-supperlattices when they are deposited from the solution by the controlled evaporation, the elongated core-shell NQDs tend to align randomly regarding to each other and lack long range orders in the thin film. This is reflected by the blurring of the diffraction rings in the selected-area-electron-diffraction (SAED) patterns of core-shell nanocrystals revealing the misorientation of the c-axes in the deposited nanoparticle-thin films (Fig. 3). The same trend was also reported for II-VI core-shell NQDs [17]. The observed aspect ratio in the NQD shape upon multi-layer shell coverage is possibly due to the preferred shell growth along certain crystal directions when the shell thickness is beyond certain number of atomic layers.

X-ray Photoelectron Spectroscopy (XPS) analysis on the core-shell NQDs was performed on a modified Kratos XSAM 800 pci using Mg K□ radiation (1253.6 eV) with an x-ray voltage of 12 kV, a current of 20 mA, and a pass energy of 20 eV. The XPS data was collected in high resolution mode with a step size of 0.2 eV with dwell times varying to obtain a reasonable signal to noise ratio. Both plain core PbSe nanocrystals and nanocrystals overcoated by four monolayers of PbS shells were examined by XPS. It has been found that both Se_{3P} and S_{2P} peaks are detectable in the XPS spectrum of core-shell structures whereas only the Se_{3P} peak appears in the spectrum of bare dot structure. This directly indicates the overcoating of the selenium compound core with the sulfide based shell layer.

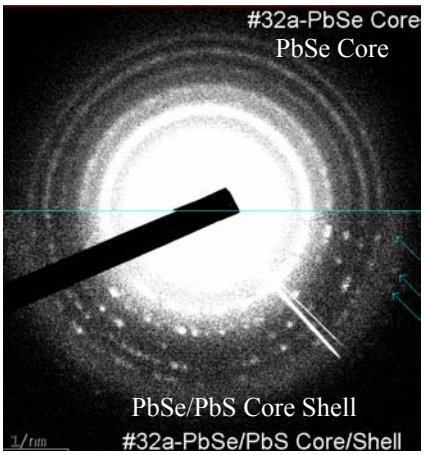

Figure 3. Selected-area-electron-diffraction (SAED) patterns of plain core PbSe (upper half) and core-shell PbSe-PbS nanocrystals

The processibility of the core-shell NQDs was investigated by conducting ligand exchange on the nanocrystal surfaces and studying the photoluminescence properties of the surface-engineered core-shell nanoparticles in comparison with their plain core counter parts. While the oleate ligand based synthetic approach has been developed to produce IV-VI infrared NQDs of high

quantum efficiency, the long chain nature of the "18-carbon" oleic molecules poses barriers for the charge separation and the carrier-transport at the nanocrystal surface, which substantially limit the applications of these infrared NQDs in light emitting devices and photovoltaics. Techniques such as ligand exchange and ligand removal are under investigation in order to address this problem, where the core-shell architecture of NQDs could potentially protect the light emitting core from degrading when undergoing post-synthesis chemical treatments. In this study, the oleate ligand overcoating the core-shell NQDs were replaced with short-chain "8-carbon" octadmine molecules to study the effect of the shell layer on the optical properties of the ligand exchanged NQDs.

While the details of the ligand exchange process will be reported elsewhere, a brief description is as follows. The powder of the as-prepared PbSe nanocrystals was first prepared from their solution with the methanol precipitation, centrifugation, decantation, and drying processes. The precipitated nanocrystal powder was then dissolved in a small amount of octylamine (C8H19N). After the solution was heated at 75 °C for 16 hours, and the octylamine-capped nanocrystals were immediately purified from the excess ligands by precipitation with a polar solvent, and the final precipitate was dispersed into the desired solvent for storage. Some plain-core PbSe NQDs were also ligand-exchanged with the same procedure and used as control samples in our study.

PL characterization on the ligand exchanged PbSe/PbS core-shell NQDS has revealed a peak-intensity drop of ~20% with respect to the as-synthesized core-shell ones without noticeable wavelength shift of the PL maxima. In contrast, the PL yield of the control samples, i.e. the plain core PbSe NQDs, dropped by 90% after the treatment of the ligand exchange, which was also accompanied by a slight blue-shift (~5nm) of the PL maximum. Similar decrease of the quantum yield has been observed in ligand-exchanged CdSe NQDs and has been attributed to a loss of passivation on the surface of the QD which creates new defects and opens up pathways for nonradiative relaxation. The fact that the core-shell infrared NQDs exhibit less reduction of the photoluminescence efficiency than the plain core structures after undergoing the same ligand exchange process clearly indicates that the light emitting core in the core-shell architecture are better protected by the wide band gap semiconductor shells and therefore more robust toward subsequent chemical/physical processing in their electronic/optoelectronic device applications.

4 ACKNOWLEDGMENT

J. Xu would like to thank Michael Gerhold for helpful discussions on the semiconductor quantum dots. This work was supported by the U. S. Army Research Office under Contract No. DAAD19-02-D-0001 and the Pennsylvania State University Nanofabrication Facility and the National Science Foundation Cooperative Agreement No. 0335765, National Nanotechnology Infrastructure Network, with Cornell University.

REFERENCES

[1] Timoshenko and Woinowski-Krieger, "Theory of Plates and Shells," McGraw-Hill, 415-4215, 1959.
[2] D. Snow, M. Major and L. Green, Microelectronic Engr. 30, 969, 1996.
[3] Author, "Title (optional)," Journal, Volume, Pages, Year.
[1] B. C. Murray, S. Sun, W. Gaschler, H. Doyle, A. T. Betley, and R. C. Kagan, vol. 45, no. 1, pp. 47-56, January. 2001.
[2] W. W. Yu, C. J. Falkner, S. B. Shih, and L. V. Colvin, Chemistry of Materials., 16, 3318, 2004.
[3] C. Feng, L. K. Stokes, W. Zhon,, J. Fang, and B. C. Murray, Materials Research Society Symposium – Proceedings., 691, 359, 2002.
[4] A. M. Hines, and D. G. Scholes, Advanced Materials., 15, 1844, 2003.
[5] L. B. Wehrenberg, W. Congjun, and P. Guyot-Sionnest, Journal of Physical Chemistry B., 106, 10634, 2002.
[6] K. U. Gautam, and R. Seshadri, Materials Research Bulletin., 39, 669, 2004.
[7] M. J. Pietryga, D. R.Schaller, D. Werder, H. M. Stewart, I. V. Klimov, and A. J. Hollingsworth, Journal of the American Chemical Society., 126, 11752, 2004.
[8] H. Du, C. Chen, R. Krishnan, D. T. Krauss, M. J. Harbold, W. F. Wise, G. M. Thomas, and J. Silcox, Nano Lett., 2, 1321, 2002.
[9] D. R.Schaller, A. M. Petruska, and I. V. Klimov, Journal of Physical Chemistry B., 107, 13765, 2003.
[10] S. J.Steckel, S. Coe-Sullivan, V. Bulovic, and G, M. Bawendi, Advanced Materials., 15, 1862, 2003.
[11] E. H. Sargent, Advanced Materials, 17, 515, 2005.
[12] Wehrenberg, Brian L.; Guyot-Sionnest, Philippe, Journal of the American Chemical Society, 125, 7806, 2003.
[13] Ginger, D.S.; Greenham, N.C., Journal of Applied Physics, 87, 1361, 2000.
[14] C. B. Murray and C. R. Kagan, M. G. Bawendi. Annu. Rev. Mater. Sci. 30, 545, 2000.
[15] S. Park, B. L. Clark, D. A. Keszler, J. P. Bender, J. F. Wager, T. A. Reynolds, G. S. Herman, Science 297, 65, 2002
[16] B. O. Dabbousi, J. Rodriguez-Viejo, F. V. Mikulec, J. R. Heine, H. Mattoussi, R. Ober, K. F. Jensen, and M. G. Bawendi, J. Phys. Chem. B, 101, 9463, 1997
[17] J. J. Li,.A. Wang, W. Guo, J. C. Keay, Tetsuya, D. Mishima,|M. B. Johnson,|and X. Peng, J.Am.Chem.Soc.125, 12567, 2003